AIP Journal of Applied Physics

# Molecular dynamics simulation of thermal energy transport in polydimethylsiloxane

Tengfei Luo, Keivan Esfarjani, Junichiro Shiomi, Asegun Henry, and Gang Chen

Citation: Journal of Applied Physics **109**, 074321 (2011); doi: 10.1063/1.3569862
View online: http://dx.doi.org/10.1063/1.3569862
View Table of Contents: http://scitation.aip.org/content/aip/journal/jap/109/7?ver=pdfcov
Published by the AIP Publishing

# Molecular dynamics simulation of thermal energy transport in polydimethylsiloxane (PDMS)

Tengfei Luo, Keivan Esfarjani, Junichiro Shiomi, Asegun Henry, and Gang Chen[a)]
*Department of Mechanical Engineering, Massachusetts Institute of Technology, Cambridge, Massachusetts 02139, USA*

(Received 8 November 2010; accepted 27 February 2011; published online 12 April 2011)

Heat transfer across thermal interface materials is a critical issue for microelectronics thermal management. Polydimethylsiloxane (PDMS), one of the most important components of thermal interface materials presents a large barrier for heat flow due to its low thermal conductivity. In this paper, we use molecular dynamics simulations to identify the upper limit of the PDMS thermal conductivity by studying thermal transport in single PDMS chains with different lengths. We found that even individual molecular chains had low thermal conductivities ($\kappa \sim 7$ W/mK), which is attributed to the chain segment disordering. Studies on double chain and crystalline structures reveal that the structure influences thermal transport due to inter-chain phonon scatterings and suppression of acoustic phonon modes. We also simulated amorphous bulk PDMS to identify the lower bound of PDMS thermal conductivity and found the low thermal conductivity ($\kappa \sim 0.2$ W/mK) is mainly due to the inefficient transport mechanism through extended vibration modes. © *2011 American Institute of Physics*. [doi:10.1063/1.3569862]

## I. INTRODUCTION

Thermal dissipation in microelectronic devices is an important issue which influences their performance. This issue becomes more significant as the size of the device shrinks and the power density increases. In a chip package, heat must pass through several interface materials between the die, the heat spreader and the heat sink. Among these interface materials, the polymer connecting the heat sink and the heat spreader is one of the major barriers that impede thermal transport. Despite their low thermal conductivity, polymer based thermal interface materials (TIMs), also known as thermal greases or thermal pastes, are necessary for filling the surface voids and removing air gaps between the two matching surfaces.[1]

Thermal grease is primarily made of silicone oil and thickeners with different thermally conductive particles added to increase its thermal conductivity. Polydimethylsiloxane (PDMS) is the most widely used silicone oil in industry. However, PDMS suffers from the common drawback of all polymers -low thermal conductivity (~0.15 W/mK) (Ref. 2). Even with particle loading, PDMS-based thermal greases have thermal conductivity ranging from 0.7–3 W/mK with the highest being only about 5 W/mK with silver particles.[3] Therefore, understanding thermal transport in PDMS is critical to improve thermal interface materials.

Although it is known that PDMS has very low thermal conductivity, detailed study of its thermal transport properties has been rare.[4] It has been reported recently that single polyethylene (PE) chain can have very high or even divergent thermal conductivity along the chain length direction,[5,6] despite similar low thermal conductivity of its amorphous counterpart to that of PDMS. It will be interesting to find out whether the low thermal conductivity of bulk PDMS is due to the amorphous structure disorder or the intrinsically low thermal conductivity of the PDMS chains themselves. If PDMS naturally has high thermal conductivity in the form of straight chains, efforts can be made to engineer structures favorable for thermal transport similar to the structural engineering accomplished with PE.[7]

In this work, we use nonequilibrium molecular dynamics (NEMD) simulation to systematically calculate the thermal conductivity of different PDMS structures from single chain to amorphous bulk form. Different analyses are carried out to study thermal transport mechanisms. The simulations are carried out using large-scale atomic/molecular massively parallel simulator (LAMMPS).[8] Due to the presence of the fast vibrating hydrogen atoms, a small time step of 0.25fs is used. The condensed-phase optimized molecular potentials for atomistic simulation studies (COMPASS) potential was used, which has been optimized for PDMS by fitting to *ab initio* calculations.[9–11] Unlike some other polymer potentials that use harmonic bond interactions, COMPASS uses anharmonic bonding terms, making it preferred for our thermal transport study since anharmonicity is fundamentally linked to umklapp phonon scatterings processes.

## II. SINGLE PDMS CHAIN

Henry and Chen[5,6] showed that a single PE chain can have much higher thermal conductivity than its amorphous counterpart, which sets an upper limit on the thermal transport. Similarly, the maximum thermal conductivity of PDMS can be attained from the isolated single chain structure. To construct the single chain simulation supercell, we start with the basic segment of a PDMS molecule, which consists of two silicon atoms, two oxygen atoms and four methyl ($CH_3$) groups [see Fig. 1(a)]. The optimized unit cell has a length

[a)]Author to whom correspondence should be addressed. Electronic mail: gchen2@mit.edu.

 

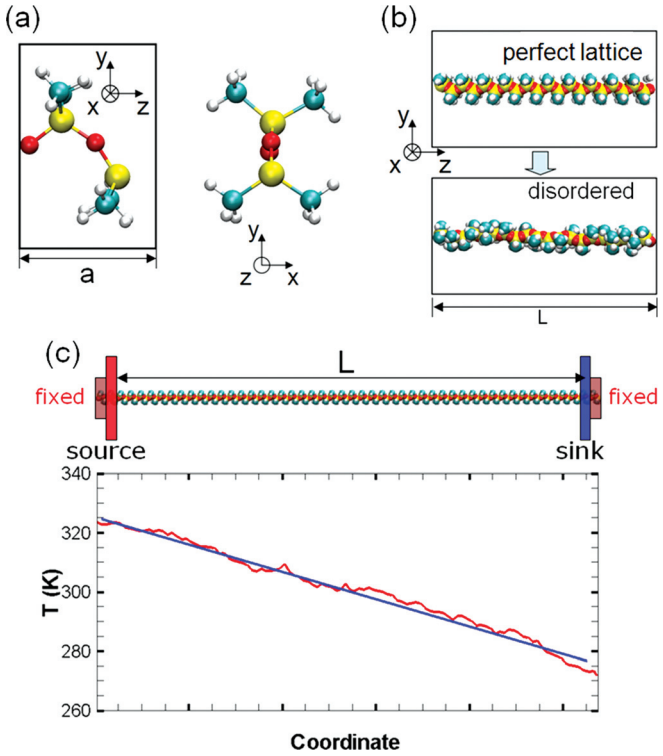


FIG. 1. (Color online) Structure plot of (a) side-view and cross-sectional view of a unit segment of PDMS, (b) a supercell of perfect and disordered single-chain PDMS, and (c) an example NEMD setup and temperature profile with source temperature set to 325 K and sink temperature set to 285 K. (O–red, Si–yellow, C–blue, H–white).

of about 5.0Å in the $z$-direction. The supercell for a single-chain PDMS is obtained by replicating the segment in the $z$-direction [see Fig. 1(b)].

To calculate thermal conductivity, we fixed the temperatures at the two ends of the sample using Langevin thermostats[12] to establish a temperature gradient across the simulation supercell [Fig. 1(c)]. Energies added into the heat source and subtracted from the sink are recorded, and used to calculate the heat flux. When steady state is attained, thermal conductivity is calculated using $\kappa = -(J/dT/dz)$, where $\kappa$ is thermal conductivity, $J$ is heat flux and $dT/dz$ is temperature gradient, which is obtained by fitting the linear part of the temperature profile. It should be noted that for an isolated single-chain, volume and cross-sectional area are not well defined. We then use the effective volume of one PDMS chain in the amorphous state as the volume of a single chain. For example, an amorphous PDMS with a density of 0.92 g/cc consisting of eight 25-segments chains has a total volume of $5.37 \times 10^4$ Å$^3$. Thus a 25-segment single chain has an effective volume of $(5.37 \times 10^4/8) = 6.72 \times 10^3$Å$^3$, yielding an effective cross- sectional area of 27 Å$^2$. In NEMD simulations, when subject to thermostats, such as Nose- Hoover and Langevin thermostats, the heat sink and source regions are attached to fictitious heat reservoirs to maintain their temperatures. These fictitious reservoirs can give raise to artificial phonon distribution, which is different from the intrinsic phonon distribution of the materials, in the sink and source regions. Due to this mismatch of frequency spectra, there can be distorted temperature profiles near the sink and source region which lead to artificial boundary effects. Depends on the nature of the boundaries, thermal transport in the systems can be influenced to different extends.[13] To avoid these artifacts introduced by the thermostats, we excluded the part of the temperature profiles near the sink and source regions, and took only the linear part of the profile to obtain the temperature gradient for thermal conductivity calculation [Fig. 1(c)].

The unphysical phonon distribution from the sink and source regions can sometimes affect a large distance from the sink and source regions, if there is not enough phonon scattering to recover the correct distribution. This is especially a problem for high thermal conductivity materials (e.g. Si), which have long phonon mean free paths. However, for materials which have low thermal conductivity and strong phonon scattering, this effect will be small. To gain confidence on our NEMD setup, we did extensive tests and comparisons on a 200 segment with a chain length ($L$) of 100 nm by using Nose-Hoover thermostats[14,15] to fix the source and sink temperature ($\kappa = 2.30$ W/mK), the reversed-NEMD scheme[16] ($\kappa = 2.10$ W/mK), fixed heat flux through velocity scaling ($\kappa = 2.21$ W/mK), and by changing the sink and source region lengths $d$ ($\kappa = 2.22$, 2.44, 2.38 W/mK for $d = 3$, 6, 9 nm, respectively). The Langevin thermostat method yields a $\kappa = 2.36$ W/mK. The variance in thermal conductivity among different methods is less than 16%, which does not influence the discussion of the results in the following contents.

We calculated thermal conductivities for system with different chain lengths at 300 K, and the results are presented in Fig. 2(a). During simulation, we found that the structure of the perfect crystalline PDMS chain became disordered easily by segment random rotation [see Fig. 1(b)]. For thermal transport, such disorder adds additional scattering to thermal carriers besides the intrinsic umklapp scattering. Due to the strong conformational disorder scattering, one would not expect the thermal conductivity of the amorphous PDMS chain to have large value. Our results show that single chain PDMS keeps increasing even up to 1600 segments ($L = 800$ nm), though the thermal conductivity remains low compared to PE.[5,6,17] It is possible that some long wavelength modes are not significantly influenced by the local conformational disorder and can still transport ballistically. It can be shown, through Boltzmann transport equation and the Matthiessen's rule, that the inverse of the thermal conductivity ($1/\kappa$) and the inverse of the sample length (1/L) have linear relationship. When we plot $1/\kappa$ against 1/L, we can obtain the intrinsic thermal conductivity of an infinitely long chain by linearly extrapolating the data to $1/\mathrm{L} = 0(\mathrm{L} = \infty)$ [see Fig. 2(b)], and the thermal conductivity comes out to be 7.2 W/mK. As a comparison, we also used equilibrium molecular dynamics (EMD) with Green-Kubo method[18] to calculate the intrinsic thermal conductivity of single chains. In the EMD simulations, periodic boundary conditions in the chain-length directions are used, making the systems equivalent to chains with infinite lengths, except for the size effect induced by the cutoff phonon wavelength which equals to the simulation supercell size. To study this size effect, we performed EMD on supercells with different lengths and plotted the calculated thermal conductivity as a function of the cell length [see Fig. 2(c)].

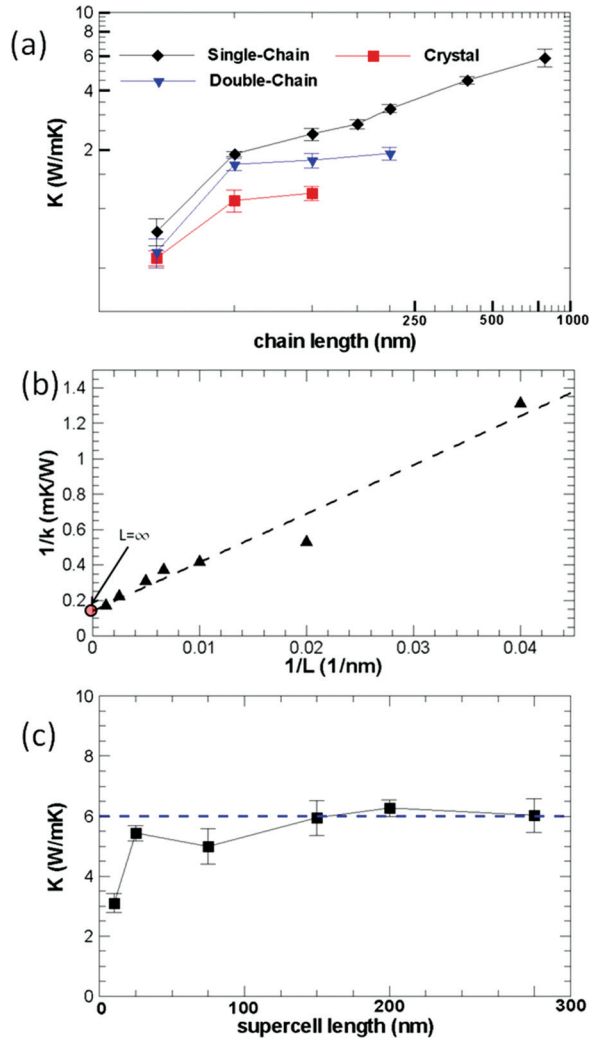


FIG. 2. (Color online) (a) Thermal conductivity of single chain PDMS as a function of the chain length from NEMD, (b) inverse thermal conductivity of single chain PDMS plotted against the inverse chain length, showing a linear dependence. Extrapolation of the line leads to the thermal conductivity of an infinitely long chain (dashed line). (c) Thermal conductivity of single chain PDMS as a function of the supercell length from EMD.

An ensemble averaging over 50 runs with different initial conditions were performed to obtain each thermal conductivity datum. More detailed description of the EMD simulations can be found in various references, such as Ref. 19. As we can see, the calculated thermal conductivity converged to 6W/mK with respect to supercell length. Thus, the intrinsic thermal conductivities from both NEMD and EMD reasonably agree with each other.

## III. CONFORMATIONAL DISORDER SCATTERING

As we can see from Fig. 2(a), the thermal conductivities of the conformationally disordered PDMS chains are small. As a comparison, a single molecular chain of PE, which has a very rigid conformation, has a much higher thermal conductivity (~350 W/mK) (Ref. 6) than those of PDMS chains, even though its phonon group velocity (~16000 m/s) is only about three times higher than that of PDMS (~5600 m/s). Thus, we believe that the conformational disorder scattering in PDMS has a large impact on the intra-chain thermal transport and lead to a significant reduction in thermal conductivity. Such disorders, introduced by the random rotations of the segments, lead to situations in which defining equilibrium atomic positions are not possible. In order to characterize the segment rotation, we calculated the backbone (Si-O-Si-O) dihedral angle probability distribution of a single PDMS chain (see Fig. 4). Very different from the sharp distribution profile of stiff polymers, like polyethylene oxide,[20] the Si-O-Si-O dihedral angle has a wide-spread distribution. Such a feature indicates the rotational softness of the PDMS backbone about the chain axis which is the result of the very flat torsional potential surface of the Si-O-Si-O dihedral angle.[10]

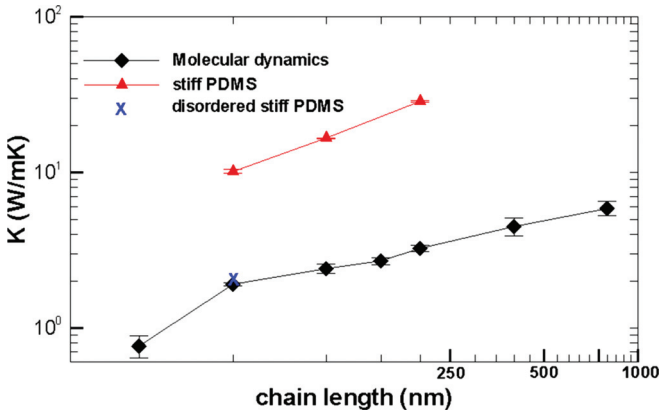


FIG. 3. (Color online) Single chain thermal conductivity for original PDMS, "stiff" PDMS and disordered "stiff" PDMS.

To further characterize the role of disorder scattering in PDMS thermal transport, we artificially increased the stiffness of the PDMS backbone by increasing the dihedral angle energy constants so that there is no random segment rotation during a molecular dynamic (MD) simulation. In this case, the perfect lattice structure is maintained throughout the simulation. As can be seen from Fig. 4, the probability distribution of the "stiff" backbone dihedral angle has distinct sharp peaks, suggesting that the temporal rotational movement of the backbone is restricted. The calculated thermal conductivities of these "stiff" PDMS chains (Fig. 3) are much larger than the original "soft" PDMS chains. We also performed a simulation on a "stiff," but "disordered" PDMS chain by increasing the dihedral angle energy constants of an already

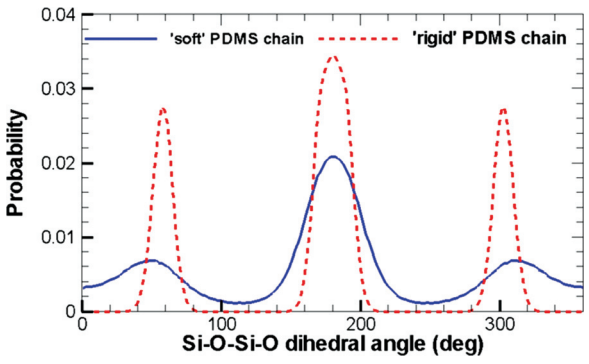


FIG. 4. (Color online) Probability distribution of Si-O-Si-O dihedral angles sampled from MD simulations.

disordered PDMS chain. In such a system, the PDMS segments are randomly rotated, but no temporal rotation can occur due to the increased dihedral angle energy constants. The thermal conductivity of this disordered "stiff" chain (cross in Fig. 3) is very close to that of the original PDMS chain. This suggests that it is the conformational disorder, instead of the temporal segment rotation, that leads to the low thermal conductivity of the single PDMS chains.

## IV. DOUBLE-CHAIN PDMS

We further simulated systems of PDMS with two chains to calculate the thermal conductivity. We also observed strong conformational disorder of the chain segments during simulations. The calculated thermal conductivity as a function of supercell length is shown in Fig. 2(a) together with the single chain thermal conductivity. Again, we used the equivalent cross-sectional areas as described in the single-chain calculations, so that the thermal conductivities of the single- and double-chain structures are directly comparable. We found that the double-chain PDMS has lower thermal conductivity and it appears to have converged within the length scale considered. The major difference between single chain and double chain PDMS is the interchain interaction, which adds extra scattering sources for phonon transport along the chains, and thus, can lead to a reduction in thermal conductivity.

## V. CRYSTALLINE PDMS

We also calculated the thermal conductivity of crystalline PDMS by simulating 8-chain supercells (see Fig. 5). Chain lengths with 50-, 100- and 200-segment long were simulated. The supercells were prepared by iterative optimizations and runs in NPT ensembles with initial arrangement illustrated in Fig. 5(b). The cross-sectional areas were about $2 \times 2$ nm. As can be seen from Figs. 5(a) and 5(c), after optimization, the chain segments are disordered and closely packed. Once the system is fully optimized in a compact pattern, there is no random rotation of chain segments as seen in single and double chain structures. The calculated thermal conductivities [see Fig. 2(a)], when converted using the equivalent cross-sectional area, are smaller than those of the single-chain and double-chain PDMS, and they saturate when the chain length exceeds 100 segments (50 nm). Compared to the double chain structure, there are more surrounding chains for each chain, thus, more scattering due to interchain interactions, which lead to lower thermal conductivities.

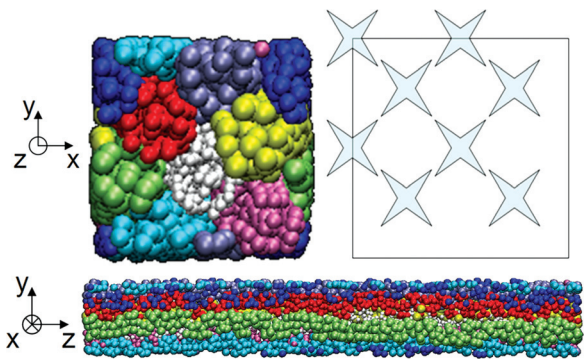


FIG. 5. (Color online) Crystalline PDMS: (a) cross-sectional view of an optimized 8-chain supercell; (b) a schematic plot of the initial configuration of the simulation box and chains; (c) side-view of the optimized supercell (8 chains are painted with different colors).

## VI. STRUCTURE INFLUENCE ON THERMAL CONDUCTIVITY

The interchain interactions, working as extra forces on chain segments, influence the motion of the chains. We found that due to the presence of the additional chains, the wavy motions of the backbone found in single chain PDMS have lower amplitude in the double-chain structure and are almost diminished in the crystalline PDMS. This observation is characterized by the gyration radius ($R_g$) of the chain backbones, which is an indication of the amplitude of the chain movement in the $x$-$y$ plane. The gyration radius is defined as

$$R_g = \sqrt{\frac{1}{M}\sum_i m_i\left[(x_i - x_{cm})^2 + (y_i - y_{cm})^2\right]},$$

where $M$ is the total mass of a PDMS chain backbone, $m_i$ is the mass of atom $i$ in the backbone, and $x_{cm}$, $y_{cm}$ are the coordinates of the center of mass. The gyration radii of the single-, double- and crystalline PMDS are $1.5548 \pm 0.0097$Å, $1.5276 \pm 0.0137$ Å and $1.4349 \pm 0.0054$ Å, respectively. This decreasing trend suggests the motions of the chains in the $x$-$y$ plane are confined when the structure changes from single chain to double chain and to crystalline PDMS. These wavy motions, corresponding to long wavelength, low frequency acoustic phonons, contribute a large amount of thermal conductivity. Suppression of these modes leads to the reduction of thermal conductivity. Such an effect can be visualized by comparing the vibrational power spectrum from single chain, double chain and crystalline structures, which is calculated by taking the Fourier transform of the velocity auto-correlation functions of the backbone atoms (Si,O) (Fig. 6).

From Fig. 6, we can clearly see the decrease in the power density of the acoustic phonons ($< 20$ cm$^{-1}$) when the structures change from single-chain to double-chain, and the power density of these modes is significantly suppressed when PDMS is in a crystalline configuration, especially in the low frequency spectrum. Such decreases in power density of acoustic modes are clearly associated with the change of the structure. For a single PDMS chain, the chain can vibrate freely due to its stand-alone structure. For the double-chain case, the vibration of each chain is restraint due to the forces from another chain. In a closely packed crystalline structure, each chain is surrounded by other chains which confine its motion to a limited space, and the long wavelength motions found in single and double chains are suppressed.

## VII. AMORPHOUS PDMS

Finally, we simulated the amorphous bulk PDMS. The modified Markov scheme[21] is used to construct the amorphous supercell with a density of 0.92 g/cc. Periodic

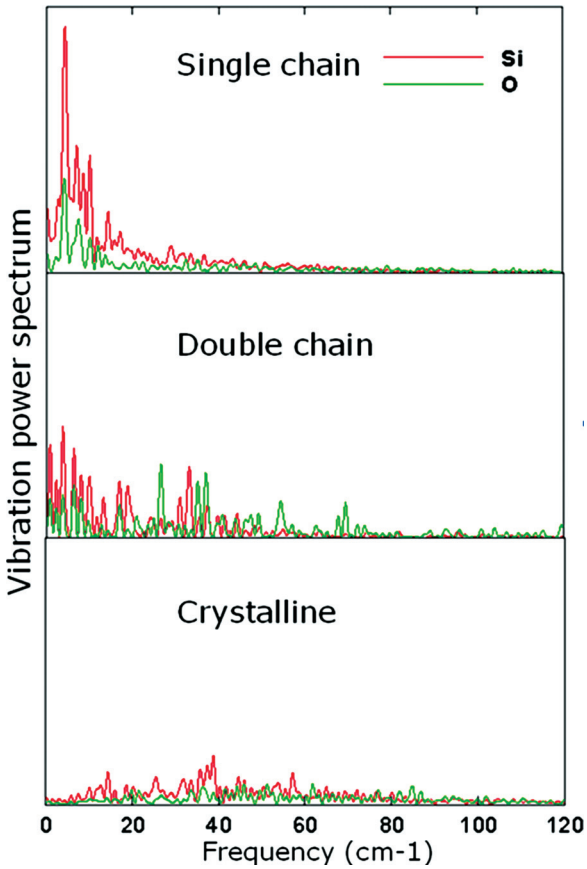


FIG. 6. (Color online) Vibration power spectrum of single-chain, double-chain and crystalline PDMS (note that only spectra up to 120 $cm^{-1}$ is shown).

boundary conditions are used in the transverse directions. Heat sink and source are placed at the ends of the supercell in the longitudinal direction (Fig. 7). The thermal conductivity is found to be around 0.2 W/mK at 300 K, which agrees reasonably with the measured value of 0.15 W/mK.[2]

In an amorphous polymer, there are three means of thermal transport: (1) ballistic transport through long wavelength propagating phonons, (2) diffusive transport through spatially extended nonpropagating vibration modes (extended modes) and (3) energy hopping among localized modes due to anharmonic transport.[22] In amorphous materials, extended

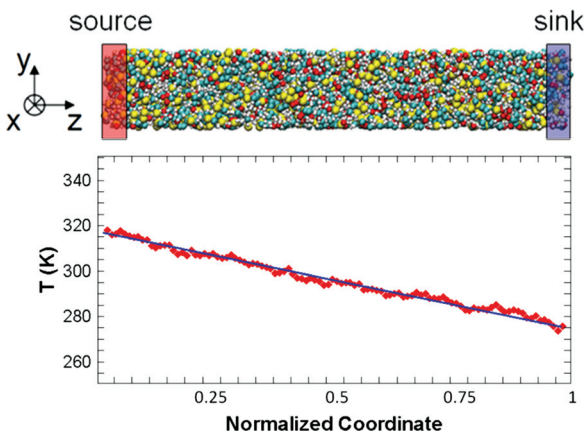


FIG. 7. (Color online) Bulk amorphous PDMS and an example temperature profile.

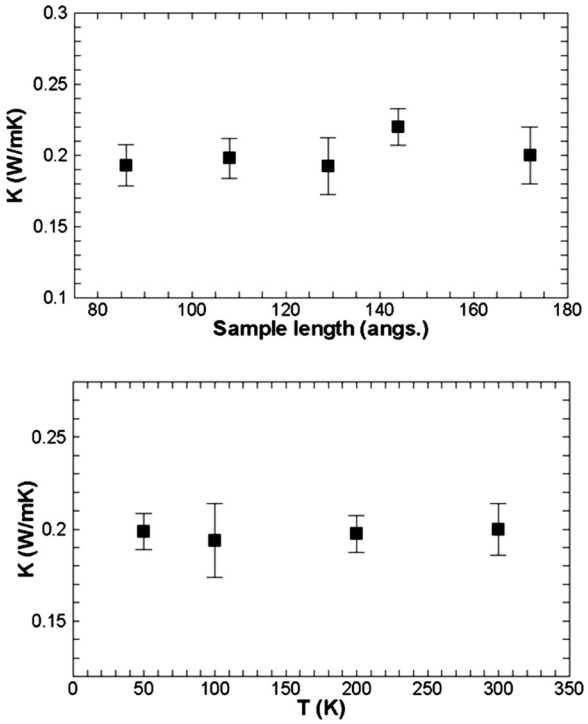


FIG. 8. (a) System size dependence and (b) temperature dependence of thermal conductivity of amorphous bulk PDMS at a constant density.

modes are usually the most important carriers for thermal transport. We also explore the roles of the other two means of transport. If the long wavelength phonons, whose mean free path are limited by boundary scatterings, dominate the transport, thermal conductivity usually increases if the simulation supercell size increases in the thermal transport direction. We calculate the thermal conductivity of samples with different lengths, and found that it is almost a constant [see Fig. 8(a)], suggesting that the ballistic transport is not important. The anharmonic energy transport among localized modes depends on anharmonicity, a feature that increases with temperature. We then calculated the temperature dependence of the amorphous PDMS thermal conductivity [see Fig. 8(b)]. To exclude possible phase change effects on thermal conductivity, the same density is used at all temperatures. We found that temperature does not have a strong influence on the thermal conductivity, suggesting that localized modes are not dominant thermal carriers.

## VIII. CONCLUSION

By using NEMD, we found that a single PDMS chain has low thermal conductivity (~6 W/mK at L = 800 nm). However, increase of thermal conductivity with chain length is still observed with chain lengths of up to 800 nm because long wavelength modes, which oversee the local disorder, can still transport ballistically. Thermal conductivities from MD of perfect "stiff" chains have much larger values compared to those from NEMD, suggesting that conformational disorder in the chain segments greatly reduce the single chain thermal conductivity. Double chain and crystalline PDMS have lower thermal conductivity than single chain structures due to interchain scattering and suppression of

acoustic phonon modes. Amorphous PDMS has a thermal conductivity of around 0.2 W/mK. Propagating modes and localized modes are found to be insignificant to thermal transport in amorphous systems. Overall, PDMS is found to have low thermal conductivities even in a single chain form, when compared to stiffer polymers such as PE. Our simulation results suggest that the low thermal conductivity is primarily due to conformational disorder within individual chains and structure disorder among collections of chains.

## ACKNOWLEDGMENTS

We would like to thank Dr. N. Yang, Dr. Y. Chalopin, Dr. J. Jin and Ms. Z. Tian for valuable discussions. This research was supported in part by National Science Foundation (Grant No. CBET-0755825), by DARPA NTI program via Teledyne, and TeraGrid resources provided by TACC Ranger (Grant No.TG-CTS100078).

[1]Z. Lin, G. S. Becker and S. M. Zhang, Compotech June **4**, 103 (2004).
[2]J. Mark, *Polymer Data Handbook* (Oxford University Press, New York 1999).
[3]E. Samson, S. Machiroutu, J.-Y. Chang, I. Santos, J. Hermarding, A. Dani, R. Prasher, D. Song, and D. Puffo, Intel Technol. J. **9**, 75 (2005).
[4]J. J. C. Picot and F. Debeauvais, Polym. Eng. Sci. **15**, 373 (1975).
[5]A. Henry and G. Chen, Phys. Rev. B **79**, 144305 (2009).
[6]A. Henry and G. Chen, Phys. Rev. Lett. **101**, 235502 (2008).
[7]S. Shen, A. Henry, J. Tong, R. Zheng, and G. Chen, Nat. Nanotechnol. **5**, 251 (2010).
[8]S. Plimpton, J. Comp. Phys. **117**, 1 (1995).
[9]H. Sun, J. Phys. Chem. B **102**, 7338 (1998).
[10]H. Sun and D. Rigby, Spectrochim. Acta, Part A **53**, 1301 (1997).
[11]H. Sun, Macromolecules **28**, 701 (1995).
[12]T. Schneider and E. Stoll, Phys. Rev. B **17**, 1302 (1978).
[13]A. Kundu, A. Chaudhuri, D. Roy, A. Dhar, J. L. Lebowitz and H. Spohn, Europhys. Lett. **90**, 40001 (2010).
[14]S. Nose, J. Chem. Phys. **81**, 511 (1984).
[15]W. G. Hoover, Phys. Rev. A **31**, 1695 (1985).
[16]F. Muller-Plathe and D. Reith, Comp. Theor. Polym. Sci. **9**, 203 (1999).
[17]A. Henry, G. Chen, S. J. Plimpton, and A. Thompson, Phys. Rev. B **82**, 144308 (2010).
[18]R. Kubo, M. Yokota and S. Nakajima, J. Phys. Soc. Jpn. **12**, 1203 (1957).
[19]T. Luo and J. R. Lloyd, J. Heat Transfer **132**, 032401 (2010).
[20]J. Ennari, I. Neelov, F. Sundholm, Polymer **41**, 4057 (2000).
[21]M. P. Allen and D. J. Tildesley, *Computer Simulation of Liquids* (Oxford University Press, New York, 1987).
[22]P. B. Allen and J. L. Feldman, Phys. Rev. Lett. **62**, 645 (1989).